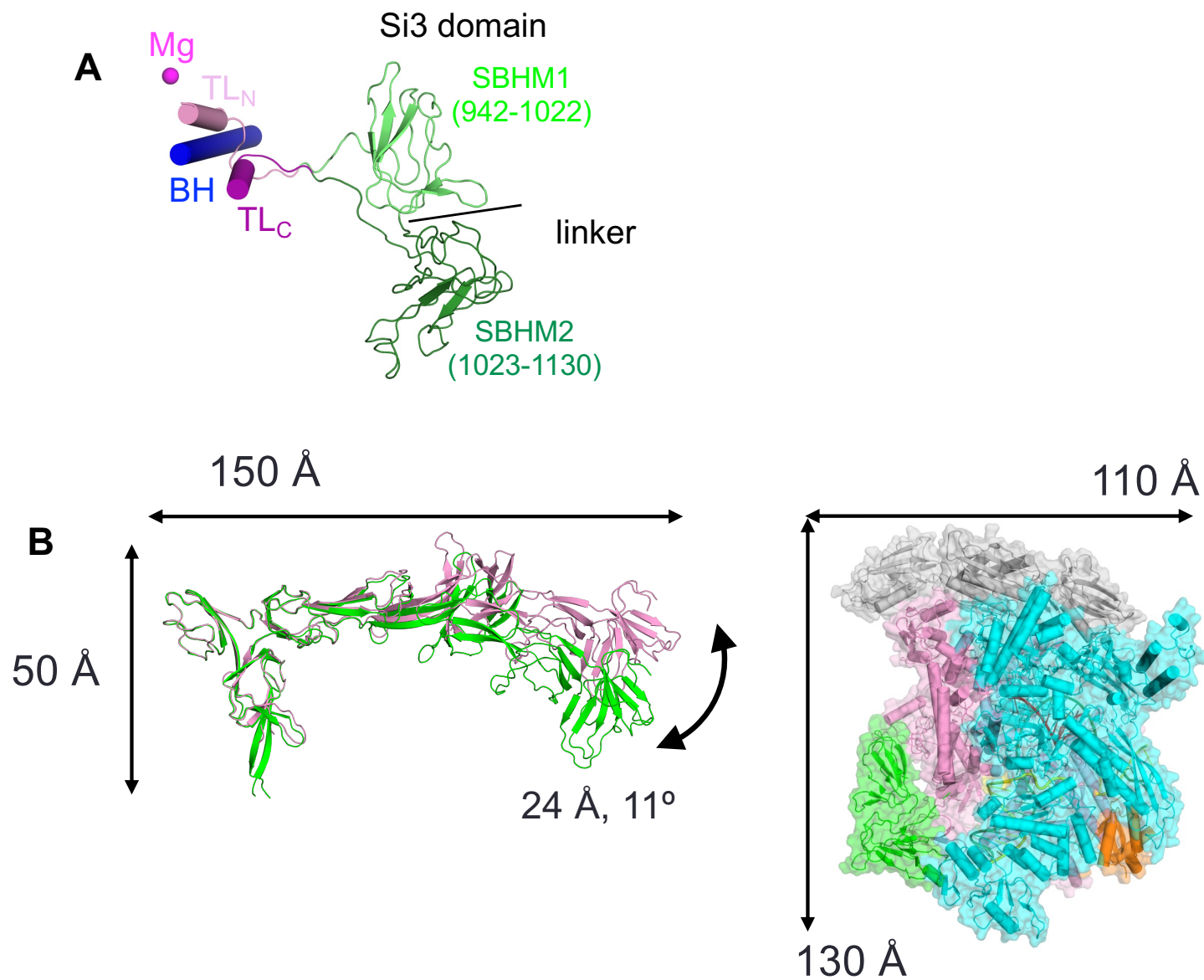
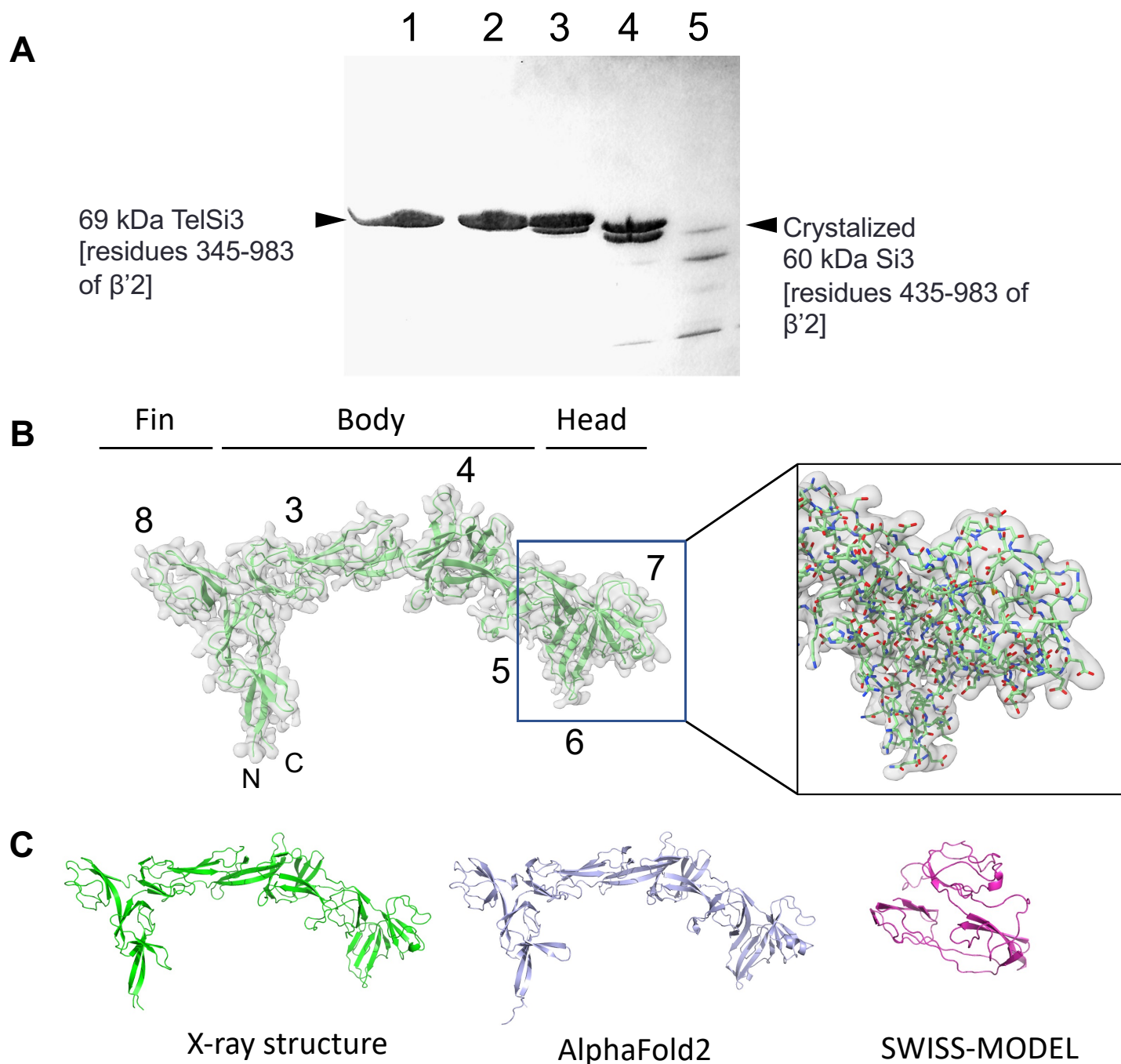


SFig. 1



SFig. 1. (A) Structure of the Si3 domain (light and dark green) of *E. coli* RNAP, its connection to the trigger loop (TL). Mg²⁺ bound at the active site and bridge helix (BH) are depicted as a sphere and cartoon models. (C) Comparing the sizes of Si3 domain (without Tail sub-domain, SBHM1) of cyanobacterial RNAP and the *E. coli* RNAP (Si3 of the *E. coli* RNAP is highlighted in green).

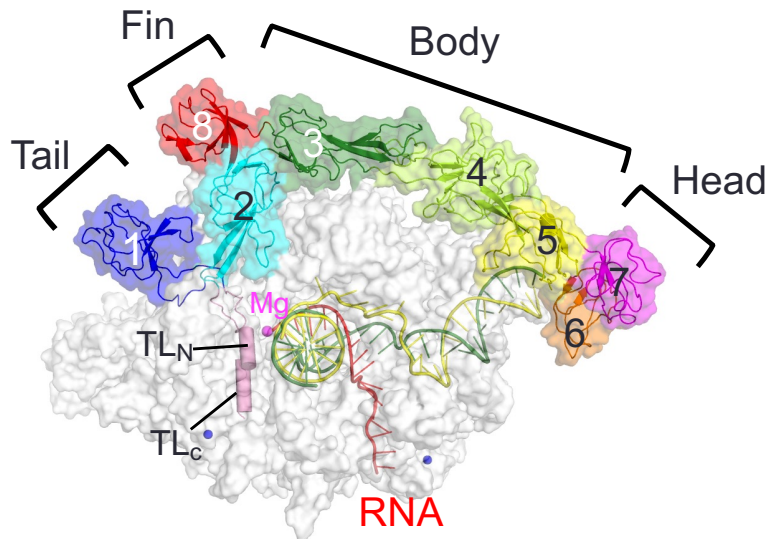
SFig. 2



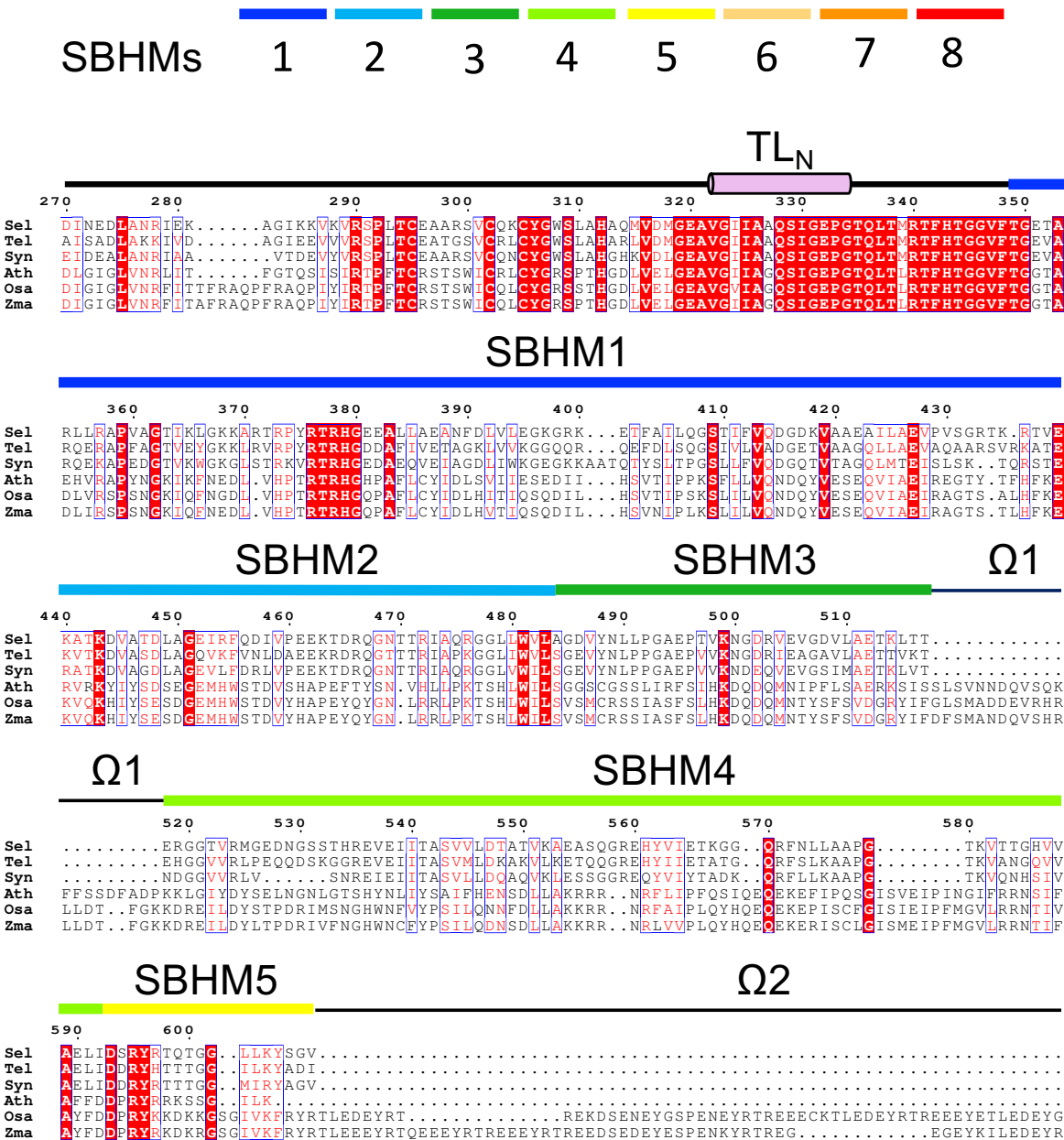
SFig. 2. (A) Limited trypsinolysis of the TelSi3 protein analyzed by SDS-PAGE. Reactions contained 10 mg/ml of TelSi3 and 0, 5, 50, 500 and 5000 nM of trypsin (lanes 1 to 5, respectively). (B) $2F_o-F_c$ electron density map of the TelSi3d Δ N (gray transparent, σ cutoff=1.3) overlaid on a protomer I in an asymmetric unit (green cartoon model). The SBHM are labeled (2 to 8) and sub-domains are indicated. Magnified view of a boxed area is shown with a stick model of the TelSi3d Δ N (Head sub-domain). (C) Comparing the X-ray structure of TelSi3d Δ N (left) with the structures predicted by AlphaFold2 (middle) and SWISS-MODEL (right).

SFig. 3

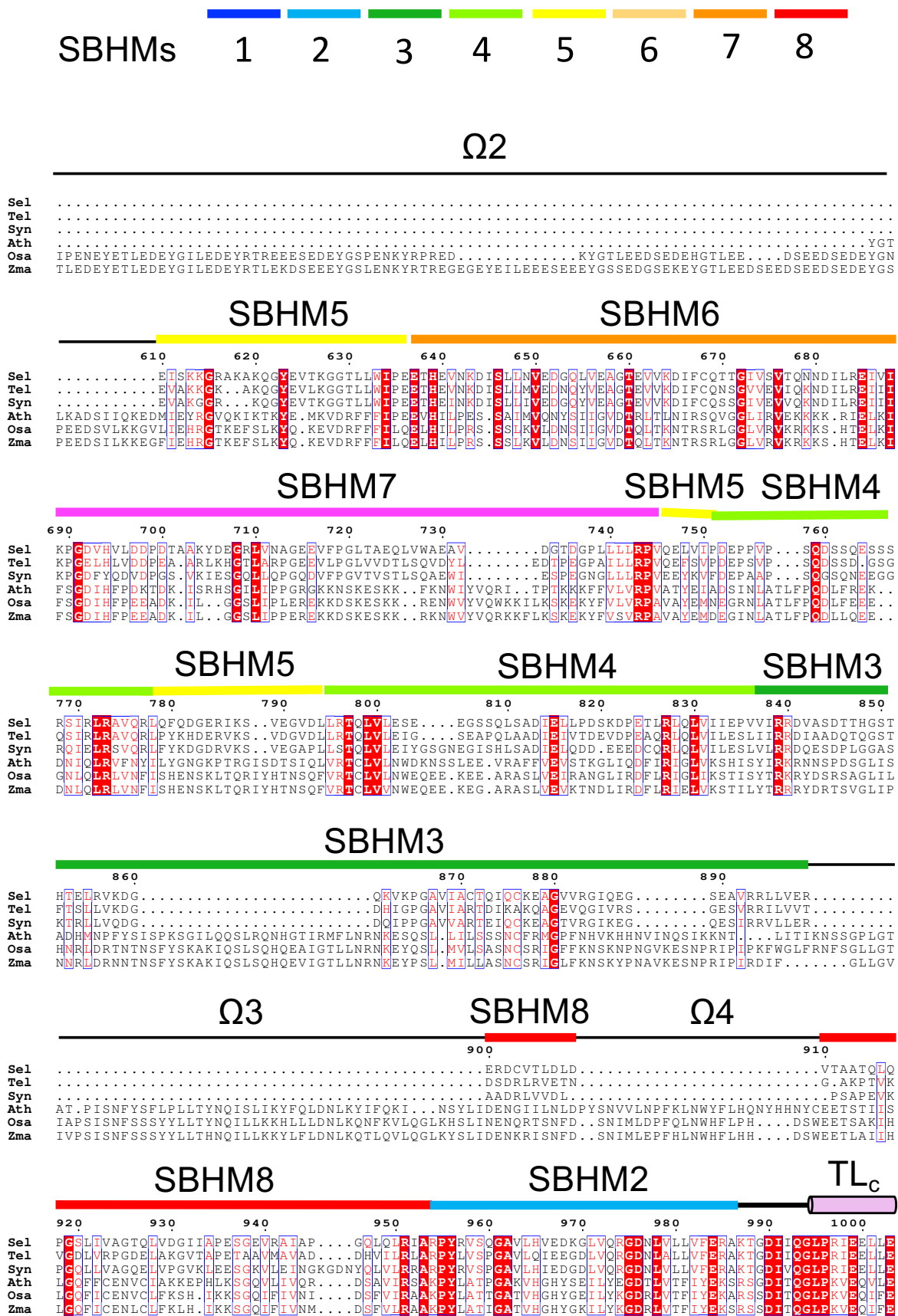
A



B



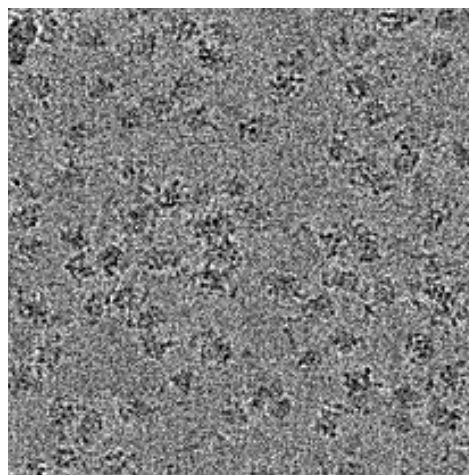
SFig. 3



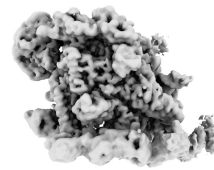
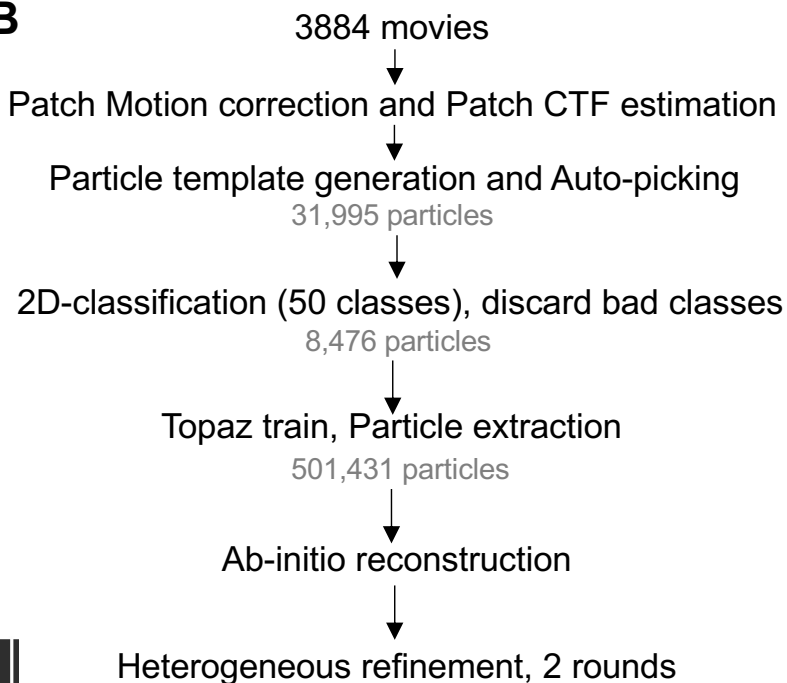
SFig. 3. Si3 structure and sequence alignment. (A) The structure of elongation complex with NusG are shown as transparent surface, and the Si3, DNA/RNA and trigger loop (TL_N, TL_C) are shown as cartoon models. The SBHM are labeled 1 to 8 and sub-domains (Tail, Fin, Body and Head) are indicated. The active site of RNAP is indicated as it coordinating Mg²⁺ (magenta sphere). (B) Sequence alignment comparing cyanobacterial Si3 (Sel, *Synechococcus elongatus*; Tel, *Thermosynechococcus elongatus*; Syn *Synechocystis* sp. PCC 6803) with the corresponding inserts from chloroplast RNAP of plant (Ath, *Arabidopsis thaliana*; Osa, *Oryza sativa*; Zma, *Zea mays*). The identical and conserved sequences are indicated by red background and red text, respectively. The sequence alignment was performed using Clustal-Omega (44) and visualized by Endscript 2.0 (45). The number scale above the sequences corresponds to the Sel sequence. Insertions found in chloroplast Si3 domains are indicated by Ω.

SFig. 4

A



B

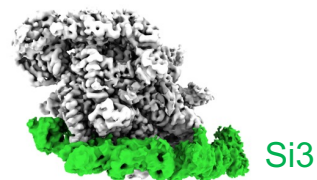


TEC-NusG

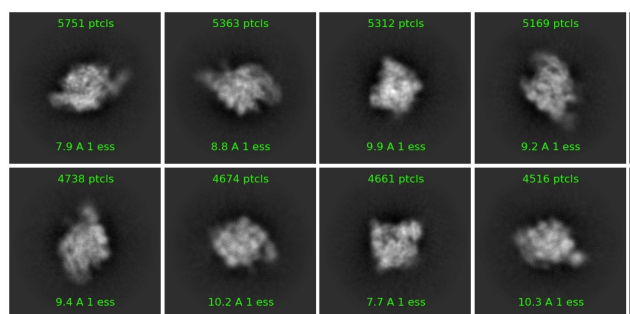
176,309 particles

Local motion correction

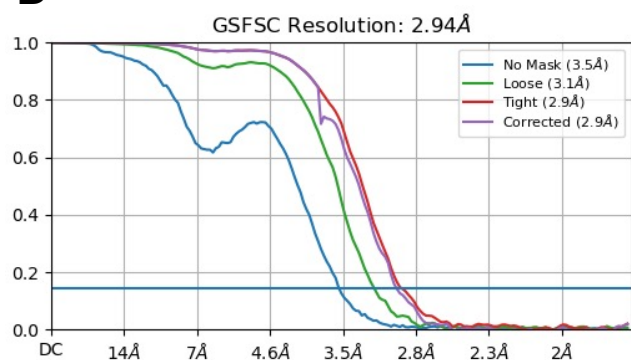
Non-uniform refinement, 2.94 Å



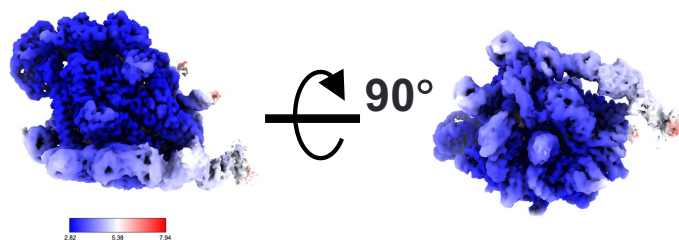
C



D

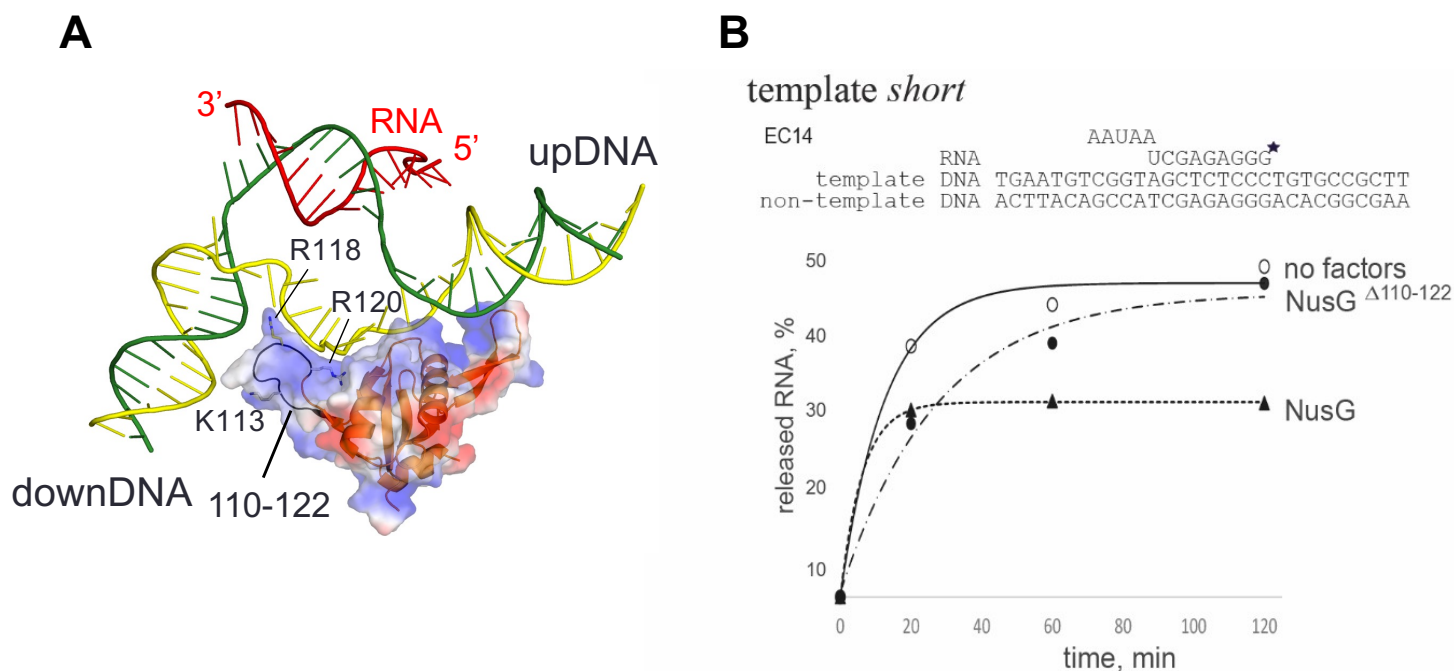


E



SFig. 4. Cryo-EM processing pipeline of the cyRNAP elongation complex with NusG. (A) A representative micrograph used for data processing. (B) Cryo-EM data processing and classification flow chart. (C) Selected representative 2D classes. (D) Fourier shell correlation (FSC) plot for half-maps with 0.143 FSC criteria indicated. (E) Local resolution maps.

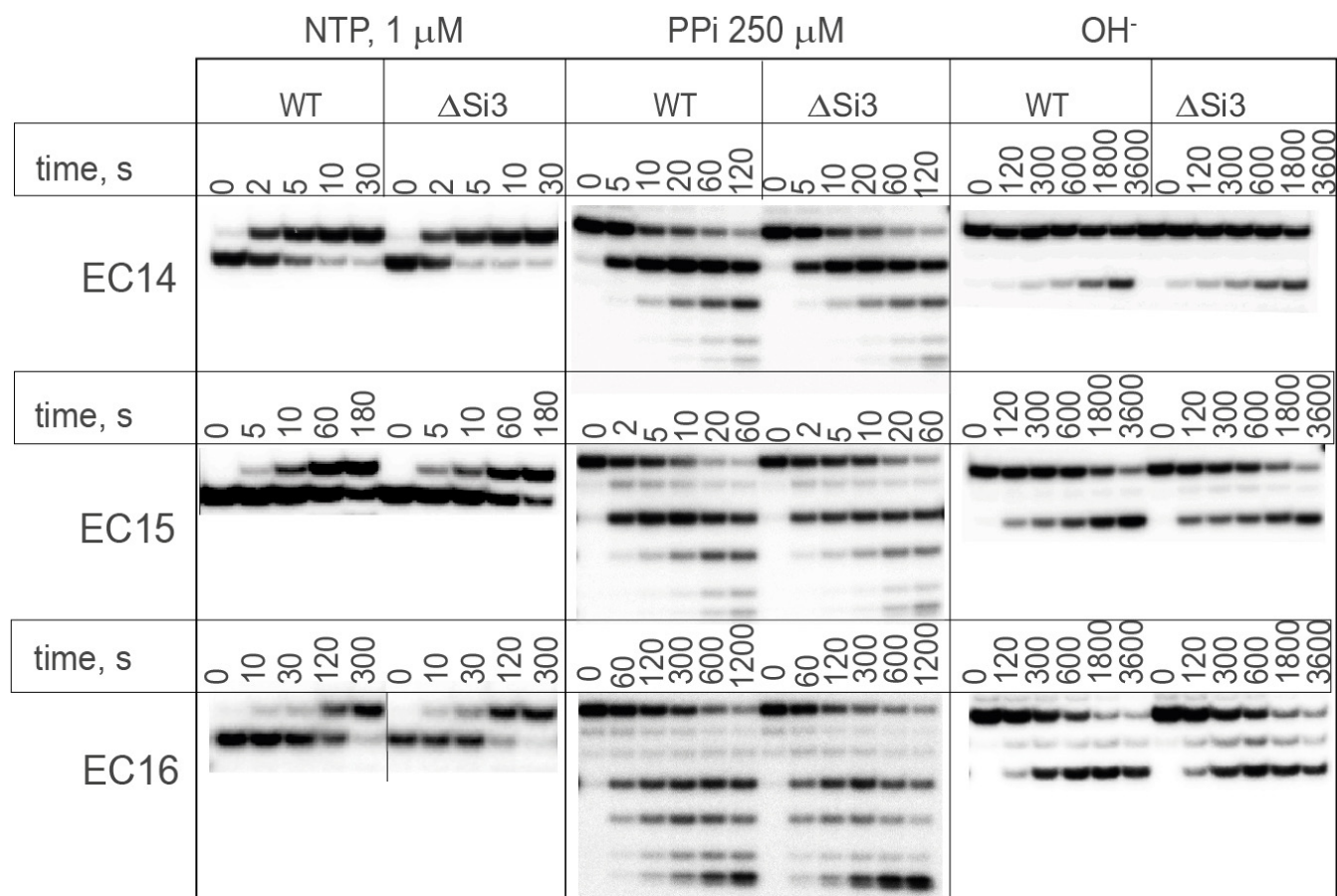
SFig. 5



SFig. 5. Structure and function of cyanobacterial NusG. (A) NusG interaction with DNA. DNA/RNA scaffold and NusG (orange) from the EC-NusG are depicted with cartoon models with transparent surface of NusG showing its electrostatic potential (blue and red, positive and negative). A unique loop of cyanobacterial NusG (residues 110-112) is indicated by black. (B) NusG increases stability of cyRNAP elongation complex. Elongation complex was assembled using oligo DNA and RNA shown above the plot, and immobilized on Ni-NTA sepharose beads via His6 tag on RNAP. Plot shows kinetics of RNA release from the elongation complexes challenged with 300 mM NaCl, in percentage from total initial amount of RNA in complex.

SFig. 6. Cryo-EM processing pipeline of the iNTP bound cyRNAP elongation complex with NusG. (A) A representative micrograph used for data processing. (B) Cryo-EM data processing and classification flow chart. (C) Fourier shell correlation (FSC) plot for half-maps with 0.143 FSC criteria indicated. (D) The structure of active site of iNTP bound EC overlaid with cryo-EM map of DNA, RNA, iNTP and Mg (gray transparent). (E) The sequence of DNA/RNA scaffold used for preparing the iNTP bound EC-NusG (template DNA, green; non-template DNA, yellow; RNA, red). 3'-deoxy modified RNA was prepared by extending RNA with 3'-deoxy ATP after assembled EC with cyRNAP, DNA/RNA and NusG. DNA and RNA regions lacking cryo-EM density are underlined.

SFig. 7



SFig. 7. Activity of WT and Δ Si3 cyRNAPs. Kinetics of single NTP incorporation, pyrophosphorolysis and phosphodiester bond hydrolysis (dinucleotide cleavage) in EC14, EC15 and EC16. Representative gels are shown. Related to Fig 4C.

SMovie 1. Cryo-EM density map of the cyRNAP elongation complex with NusG.

Related to Fig. 2B.

SMovie 2. Conformational changes of trigger loop/helix, rim helix and Si3 during the

iNTP binding at the active site. Related to Fig. 4B.

Supplemental Table 1. X-ray crystallographic data collection and structure refinement statistics of the TeISi3ΔN

PDB code	8EMB		
Data collection		Refinement	
Space group	P3(2)21	Resolution (Å)	50–3.06 (3.10-3.06)*
Cell dimensions		R_{work}	0.249 (0.387)*
a (Å)	178.663	R_{free}	0.278 (0.371)*
b (Å)	178.663	No. of atoms	21,086
c (Å)	281.038	No. of waters	0
α, β, γ (°)	90, 90, 120	R.m.s deviations	
Resolution (Å)	50–3.07 (3.12-3.07)*	Bond length (Å)	0.014
Total reflections	1,165,515	Bond angles (°)	1.557
Unique reflections	96,754 (4,161)*	Clashscore	17.63
Redundancy	12.0 (9.5)*	Ramachandran favored, %	91.97
Completeness (%)	98.9 (85.8)*	Ramachandran outliers, %	0.07
I / σ	17.0 (0.74)*		
$CC^{1/2}$	0.999 (0.645)*		
No. of Se sites	44		
FOM	0.753		

*Highest resolution shells are shown in parentheses

Supplementary Table 2. Cryo-EM data collection, refinement and validation statistics

	EC-NusG (EMD-40874) (8SYI)	EC-NusG_CTP (EMD- 42502) (8URW)
Data collection and processing		
Magnification	75,000	105,000
Voltage (kV)	300	300
Electron exposure (e ⁻ /Å ²)	45	40
Defocus range (μm)	-0.75 to -2.5	-0.75 to -1.75
Pixel size (Å)	0.87	0.855
Symmetry imposed	C1	C1
Initial particle images (no.)	501,431	414,959
Final particle images (no.)	176,309	132,172
Map resolution (Å)	2.94	2.79
FSC threshold	0.143	0.143
Map resolution range (Å)	2.82 -11.48	2.47 - 8.67
Refinement		
Initial model used (PDB code)	8EMB, 8GZG	
Model resolution (Å)	2.94	2.79
FSC threshold	0.143	0.143
Map sharpening <i>B</i> factor (Å ²)	-109	-53.4
<i>Model composition</i>		
Non-hydrogen atoms	29,500	29,896
Protein residues	3,537	3,574
Nucleic acid residues	91	94
Ligands	Zn:2, Mg:1	Zn:2, Mg:1
<i>B factors (Å²) (mean)</i>		
Protein	71.71	106.22
DNA/RNA	171.97	195.73
Ligand	100.75	61.08
<i>R.m.s. deviations</i>		
Bond lengths (Å)	0.005	0.003
Bond angles (°)	0.644	0.562
<i>Validation</i>		
MolProbity score	2.46	2.26
Clash score	6.85	6.27
Rotamer outliers (%)	6.09	4.41
<i>Ramachandran plot</i>		
Favored (%)	91.95	93.54
Allowed (%)	7.74	6.12
Disallowed (%)	0.31	0.34